Kobe University Repository : Kernel

PDF issue: 2025-12-05

Polarization characteristics of electroluminescence and net modal gain in highly stacked InAs/GaAs quantum-dot laser devices

Suwa, Masaya
Andachi, Takaya
Kaizu, Toshiyuki
Harada, Yukihiro
Kita, Takashi

(Citation)
Journal of Applied Physics,120(13):134313-134313

(Issue Date)
2016-10-07

(Resource Type)
journal article

(Version)
Version of Record

(Rights)
©2016 AIP Publishing. This article may be downloaded for personal use only. Any other use requires prior permission of the author and AIP Publishing. The following article appeared in Journal of Applied Physics 120(13), 134313 and may be found at http://dx.doi.org/10.1063/1.4964446

(URL)
https://hdl.handle.net/20.500.14094/90004053

Polarization characteristics of electroluminescence and net modal gain in highly stacked InAs/GaAs quantum-dot laser devices

Masaya Suwa, Takaya Andachi, Toshiyuki Kaizu, Yukihiro Harada, and Takashi Kita

Citation: Journal of Applied Physics **120**, 134313 (2016); doi: 10.1063/1.4964446
View online: http://dx.doi.org/10.1063/1.4964446
View Table of Contents: http://aip.scitation.org/toc/jap/120/13
Published by the American Institute of Physics

Articles you may be interested in

Polarization-insensitive optical gain characteristics of highly stacked InAs/GaAs quantum dots
Journal of Applied Physics **115**, 233512 (2014); 10.1063/1.4884228

Polarization control of electroluminescence from vertically stacked InAs/GaAs quantum dots
Applied Physics Letters **96**, 211906 (2010); 10.1063/1.3441403

Two-step photocurrent generation enhanced by miniband formation in InAs/GaAs quantum dot superlattice intermediate-band solar cells
Applied Physics Letters **110**, 193104 (2017); 10.1063/1.4983288

Broadband control of emission wavelength of InAs/GaAs quantum dots by GaAs capping temperature
Journal of Applied Physics **118**, 154301 (2015); 10.1063/1.4933182

Emission-wavelength tuning of InAs quantum dots grown on nitrogen-δ-doped GaAs(001)
Journal of Applied Physics **119**, 194306 (2016); 10.1063/1.4951719

Effect of internal electric field on InAs/GaAs quantum dot solar cells
Journal of Applied Physics **115**, 083510 (2014); 10.1063/1.4867042

JOURNAL OF APPLIED PHYSICS **120**, 134313 (2016)

Polarization characteristics of electroluminescence and net modal gain in highly stacked InAs/GaAs quantum-dot laser devices

Masaya Suwa, Takaya Andachi, Toshiyuki Kaizu, Yukihiro Harada, and Takashi Kita
Department of Electrical and Electronic Engineering, Graduate School of Engineering, Kobe University, 1-1 Rokkodai, Nada, Kobe 657-8501, Japan

(Received 31 July 2016; accepted 26 September 2016; published online 7 October 2016)

We studied the polarization anisotropy of electroluminescence (EL) and net modal gain characteristics of laser device structures containing 40 stacked InAs/GaAs quantum dot (QD) layers. The electronic coupling between the closely stacked QDs enhanced the transverse-magnetic (TM) polarization component owing to the heavy- and light-hole mixing. Thereby, the [110]-waveguide devices exhibited a laser oscillation of not only the transverse-electric (TE) but also the TM component. Laser oscillation occurred at 1137 nm from the first excited state for the 300-μm-long cavity, while it occurred at 1167 nm from the ground state for the 1000-μm-long cavity. The polarization anisotropy of the EL intensity strongly depended on the injection current density. The polarized EL intensity was almost isotropic at low injection current density. As the injection current density was increased, the TE component was gradually enhanced, which resulted in a markedly TE-dominant anisotropy above the threshold current density for laser oscillation. The net modal gains evaluated using the Hakki-Paoli method also exhibited a TE-enhanced characteristic with increasing injection current density. As the EL spectra of the TE component have an inhomogeneous broadening narrower than that of the TM component, the TE-mode intensity is likely to be enhanced by the concentration of the injected carriers. *Published by AIP Publishing.* [http://dx.doi.org/10.1063/1.4964446]

I. INTRODUCTION

Self-assembled InAs quantum dots (QDs) have attracted considerable interest for optical communication devices such as low-threshold, cooler-less direct modulation lasers,[1,2] polarization-insensitive semiconductor optical amplifiers (SOAs),[3,4] and ultrahigh-speed optical switches[5,6] operating in the near-infrared bands. These devices are required to operate not only in the optical communication wavelength bands of 1.3 and 1.55 μm but also in an extremely broad band of 1.0 to 1.3 μm expected for future high-speed and high-capacity optical communication networks. The 1.0–1.3 μm band having a broad bandwidth above 70 THz is very promising for operation.[7–10] In addition, control of the optical gain characteristics is crucial because they greatly affect the device performance. Especially, in SOA devices, the polarization anisotropy of the optical gain between the transverse electric (TE)- and transverse magnetic (TM)-polarized components induces fluctuations in the output signal amplitude. However, conventional QD devices using self-assembled InAs QDs have significant polarization anisotropy of the gain,[11] as noted for SOAs with multi-quantum-well structures because the flat shape of QDs and the strong biaxial compressive strain push the light-hole (LH) band with TM gain away from the band edge of the heavy-hole (HH) band with TE gain.[3,4] Therefore, the TE gain becomes higher than the TM gain. When the QDs are vertically stacked to achieve electronic coupling,[12–23] the wave functions are delocalized along the stacking direction, and valence-band mixing of the HH and LH states occurs. This leads to the enhancement of the TM component.[15,20,21] We have recently fabricated ridge-waveguide laser devices containing 30 or 40 layers of closely stacked InAs/GaAs QDs and investigated their polarized gain characteristics.[23] As a result, the polarization-insensitive properties of the net modal gain were observed in the wavelength region of 1.1 to 1.2 μm. In particular, the polarization insensitivity at high net modal gain is essential for SOAs. The influence of the injection current density and structural parameters of the waveguide device, such as waveguide cavity length, on the gain characteristics should be understood.

In this work, we fabricated ridge-waveguide laser devices containing 40 stacked InAs/GaAs QD layers with different cavity lengths and investigated the polarization characteristics of the electroluminescence (EL) and the net modal gain as a function of the injection current density. The [110]-waveguide devices exhibited laser oscillation in both the TE and TM components. The EL intensity and net modal gain exhibited TE-enhanced characteristics with increasing injection current density, and therefore, the threshold current density for laser oscillation was lower in the TE component than in the TM component.

II. FABRICATION OF HIGHLY STACKED InAs/GaAs QDs AND DEVICE STRUCTURES

We fabricated laser device structures containing 40 stacked InAs/GaAs QD layers using solid-source molecular beam epitaxy. The device structure was fabricated on a Si-doped n^+-GaAs(001) substrate. After growing a 150-nm-thick n^+-GaAs buffer layer doped with 2.5×10^{18} cm^{-3} of Si, a 1-μm-thick $Al_{0.3}Ga_{0.7}As$ cladding layer doped with 5.0×10^{17} cm^{-3} of Si was grown at 550 °C on the substrate. Then, the active layer containing 40 stacked InAs/GaAs QD layers was grown at 480 °C. The thickness of the active layer comprising

GaAs (113.5 nm)/stacked QD layers/GaAs (113.5 nm) was 400 nm. The growth rate and nominal thickness of InAs were 0.04 monolayers per second (ML/s) and 2.0 ML, respectively, for the first QD layer. The GaAs spacer layer thickness was 4 nm, and its growth rate was 0.8 ML/s. After growing the GaAs spacer layer, a growth interruption of 10 s was introduced, and subsequently, InAs QD layers with a reduced thickness of 1.4 MLs were alternately formed. The in-plane QD density was approximately $1.0 \times 10^{10}\,\mathrm{cm}^{-2}$. The average lateral sizes of stacked QDs along the [110] and [−110] directions were 20 nm and 30 nm, respectively, which were estimated using cross-sectional transmission electron microscopy (TEM) (see Ref. 22). Then, a 1-μm-thick Be-doped p^+-$Al_{0.3}Ga_{0.7}As$ ($1.0 \times 10^{18}\,\mathrm{cm}^{-3}$)/$p$-$Al_{0.3}Ga_{0.7}As$ ($2.0 \times 10^{17}\,\mathrm{cm}^{-3}$) cladding layer was grown at 500 °C. Finally, a thin p^+-GaAs contact layer doped with 1.3×10^{19} cm^{-3} of Be was deposited.

We fabricated a ridge waveguide edge emitting-laser device by processing a mesa structure and fabricating insulation films of SiO_2 and benzocyclobutene, a protection film containing SiN, electrodes, and a high-reflection coating with a reflectivity of 83% for the front side and 97% for the back side. The width of the ridge was 5 μm, and the cavity lengths were 300 and 1000 μm. The waveguide was along the [110] direction.

III. EL MEASUREMENTS AND CHARACTERIZATION OF OPTICAL GAIN

The emission intensity of the Fabry–Pérot resonator is given by[24]

$$I = \frac{(1-R)^2 e^{gL}}{(1-Re^{gL})^2 + 4Re^{gL}\sin^2\left(\frac{2\pi L}{\lambda}\right)} I_0, \tag{1}$$

where R is the averaged reflectivity, L is the cavity length, g is the net modal gain, λ is the wavelength in the cavity, and I_0 is the intensity of the incident light. When L is equal to an integral multiple of $\lambda/2$ and $\lambda/4$, I is maximum and minimum, respectively. The net modal gain is defined by[25]

$$g = \Gamma g_{mat} - \alpha_i, \tag{2}$$

where Γ is the optical confinement factor, g_{mat} is the material gain, and α_i is the waveguide loss. We evaluated the net modal gain by analyzing the Fabry–Pérot resonance features that appeared in the high-resolution EL spectrum obtained using the Hakki-Paoli method,[26] which is a standard method for evaluating the net modal gain of a laser device operating below the threshold current. When the maximum and minimum intensities of the Fabry–Pérot resonance given by Eq. (1) are used, the net modal gain is given by the following equation:

$$g = \frac{1}{L}\ln\left(\frac{\gamma^{\frac{1}{2}}-1}{\gamma^{\frac{1}{2}}+1}\right) + \alpha_{mirror}, \tag{3}$$

and the mirror loss is given by

$$\alpha_{mirror} = \frac{1}{L}\ln\left(\frac{1}{R}\right), \tag{4}$$

where γ is the ratio of the maximum intensity to the minimum intensity of the Fabry–Pérot resonance. The EL measurements were performed at 21 °C. The device temperature was controlled using a Peltier device. The EL signal was detected by using an optical spectrum analyzer with a high wavelength resolution of 40 pm.

IV. POLARIZATION CHARACTERISTICS IN 300-μm CAVITY-LENGTH DEVICE

First, we discuss the polarization characteristics of the EL and the net modal gain in the device with the 300-μm cavity length. Figures 1(a) and 1(b) show the Fabry–Pérot resonances of the TE- and TM-polarization components obtained using high-resolution EL measurements, respectively, as a function of the injection current density. In the [110] waveguide, the TE component is parallel to the [−110] direction corresponding to the direction of the longer axis of the QD base. When the injection current density is 100 A/cm^2, the EL spectra of both the TE and TM components exhibit peaks at around 1190 nm, which originate from the ground-state emission of the stacked QDs. In addition, bumps originating from the destructive interference caused by the multi-mode optical propagation in the waveguide[27,28] appear on the bases of the TE and TM spectra at around 1190 and 1160 nm, respectively, because the waveguide with a wide ridge tends to have several different propagation angles. The EL peak shifts towards the shorter-wavelength side with increasing injection current density, and the TM spectrum is broadened. This suggests that state filling occurs in the inhomogeneously distributed ground states of the stacked QDs. As the QDs with high-energy ground states are more likely to cause thermal carrier escape compared with the QDs with low-energy ground states at room temperature, the emission from the low-energy ground states is dominant in the low injection current condition. In the high injection current condition, the emission from the high-energy ground

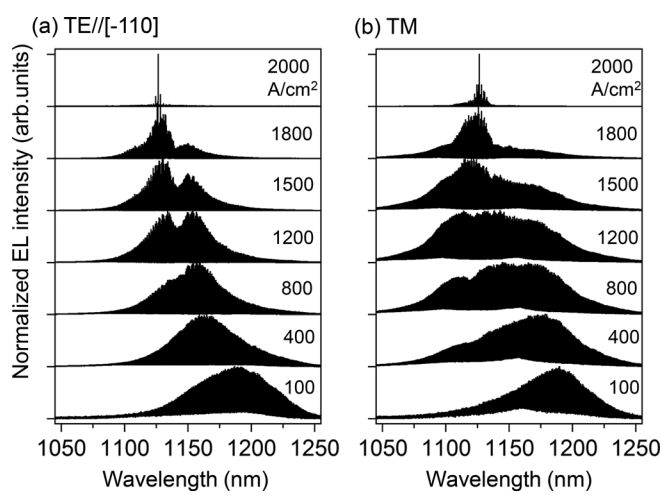

FIG. 1. Fabry–Pérot resonances of (a) the TE and (b) the TM polarization components obtained from the [−110] waveguide device with a 300-μm cavity length, as functions of the injection current density.

states also occurs because the carrier injection exceeds the thermal carrier escape. The inhomogeneity in the ground states is attributed to the height fluctuation of the stacked QDs. When the energy states of the vertically aligned QDs have an inhomogeneous distribution within the homogeneous energy width, they can be coupled and form the miniband. The magnitude of the homogeneous broadening reported in the InGaAs/GaAs QDs is 20 meV at room temperature.[29,30] On the other hand, the height of the QDs estimated from the cross-sectional TEM image is 2 to 3 nm. According to the theoretical calculation of the energy states for the truncated pyramidal InAs/GaAs QD with the base length of 13.8 nm,[31] this height fluctuation corresponds to the inhomogeneous broadening of the energy state of about 36 meV, which is larger than the homogeneous energy width. Therefore, decoupling occurs in some stacked QDs, and the actual height of the stacked QDs fluctuates in the wafer plane and/or along the stacking direction. As the highly coupled QDs emitting at the shorter wavelength exhibit remarkable TM component which is sensitive to the degree of coupling,[20] the TM spectrum extends towards the shorter wavelength side with increasing injection current density. The ground-state emission saturates above 1000 A/cm^2. Moreover, an additional peak originating from the first excited states of the stacked QDs appears on the short-wavelength side of the ground-state emission peak in the high injection current condition. The EL intensity of the first excited state increases with increasing injection current density and becomes larger than that of the ground state above 1500 A/cm^2. This bimodal feature is pronounced in the TE spectra while the TM spectra show large inhomogeneous broadening, which is attributed to a fluctuation of the stacked QD height.[32] The increase in the EL intensity of the first excited state results in laser oscillation at 1127 nm in both the TE and TM components. Generally, semiconductor laser device structures with a thin active layer do not exhibit laser oscillation of the TM component because of the low material gain due to the low optical transition probability of the TM component. In contrast, in our laser device structure, the material gain of the TM component is high enough to overcome the waveguide loss due to closely stacking QDs. Note that the enhancement of the lasing mode intensity of the TE component is greater than that of the TM component, suggesting a lower threshold current density for TE-laser oscillation.

The polarization-angle dependences of the EL peak intensities of the ground and first excited states are indicated in Figs. 2(a) and 2(b), respectively, for various injection current densities. They are represented as log-scale polar plots. The emission from the ground state is dominant at 100 A/cm^2. The polar plot of the ground-state emission shows an almost isotropic characteristic. This proves that the optical transition probability of the TM component increases because of the HH-LH mixing in the ground state induced by extending the wavefunction in stacked QDs.[20,21] Meanwhile, the enhancement of the HH-LH mixing in the ground state leads to a reduction in the ratio of the LH component contributing to the TM polarized emission in the excited state.[33,34] Therefore, the TE-polarized emission becomes dominant in the first excited state as shown in Fig. 2(b). When the injection current density

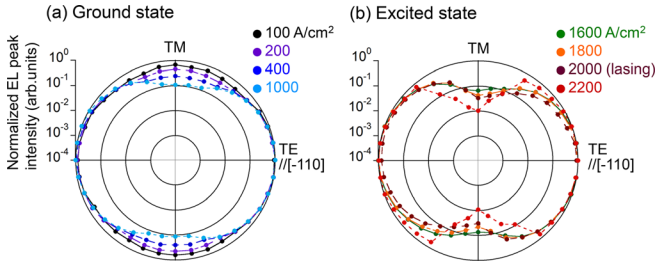

FIG. 2. Polarization-angle dependences of the EL peak intensities of (a) the QD ground and (b) the first excited state for various injection current densities, which are represented as log-scale polar plots.

is increased, the ground-state emission also exhibits the TE-polarized anisotropy. This behavior cannot be explained by the ratio of the LH component between the ground and the first excited states, reported in Ref. 28. Two more factors affecting the TE-polarized anisotropy in the ground-state emission at high injection current density are considered. One is the overlap of the ground-state emission peak with the first excited-state emission peak. The distribution of the inhomogeneous state is wider than the energy space between the ground and first excited states. In addition, the ground-state emission peak shifts towards the shorter-wavelength side with increasing injection current density, as shown in Fig. 1(a). Therefore, the ground-state emission results in the TE-dominant polarization anisotropy influenced by the first excited state. The other factor is that the increase in the mode intensity of the TE component is greater than that in the TM component. As the closely stacked QDs have lateral-size fluctuations smaller than the height fluctuations enhanced by high stacking, the inhomogeneous broadening of the EL spectra becomes narrow in the TE component, as shown in Fig. 1(a). This facilitates concentration of the injected carriers on a certain mode of the TE component, resulting in the enhanced TE emission. In addition, in the first excited-state emission, the TE-polarized anisotropy is enhanced with increasing injection current density, especially after laser oscillation. This is attributed to the threshold current density for TE laser oscillation being lower than that for TM laser oscillation, as shown in Fig. 1.

To discuss the anisotropy of the threshold current density for laser oscillation between the TE and TM components in detail, we evaluated the net modal gain by analyzing the Fabry–Pérot resonance. Figures 3(a) and 3(b) show the net modal gain spectra of the TE and TM components derived using Eq. (3), respectively, as a function of the injection current density. The gain spectra for the injection current densities less than the threshold are shown. When the injection current density is 100 A/cm^2, the TE-gain spectrum has a single peak originating from the ground state at around 1160 nm, whereas the TM-gain spectrum has a remarkable bimodal feature owing to the existence of a dip at around 1160 nm. The peak on the longer-wavelength side and the dip originate from the ground state and the destructive interference of the multi-mode optical propagation, as shown in Fig. 1, respectively. The peak gain of the TE and TM components increases with increasing injection current density and the peak positions shift towards the shorter-wavelength side. This corresponds to the behavior of the Fabry–Pérot resonance

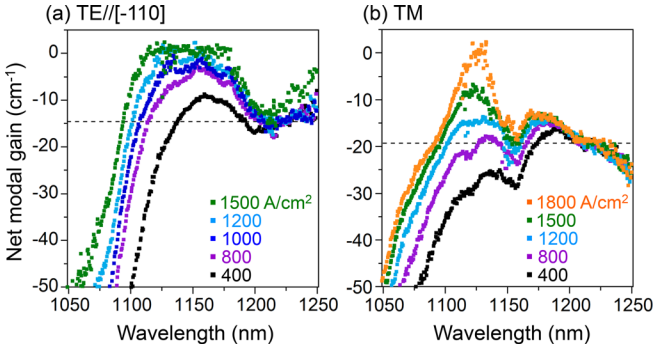

FIG. 3. Net modal gain spectra of (a) the TE and (b) the TM components derived from the Fabry–Pérot resonances in Figs. 1(a) and 1(b) by using the Hakki-Paoli method, respectively, as functions of the injection current density. The dashed lines represent the estimated waveguide losses.

spectra shown in Figs. 1(a) and 1(b). The gains of the ground state of the TE and TM components almost saturate above 800 A/cm^2. Simultaneously, the gains in the shorter-wavelength regions, originating from the first excited state, increase in both the TE and TM components. This leads to broadening of the gain spectra. The peak gains of the TE and TM components reach 0 cm^{-1} at 1200 and 1800 A/cm^2, respectively. As laser oscillation occurs when the net modal gain becomes positive, the threshold current density for laser oscillation is lower for the TE component than for the TM component. This polarization anisotropy of the gain is caused by three factors: (1) the optical confinement factor is slightly larger in the TE component than in the TM component,[23] (2) the enhancement of the material gain of the TE component owing to the concentration of the injected carriers caused by the narrow inhomogeneous mode distribution of the TE component, as mentioned in Figs. 1 and 2, and (3) the anisotropic waveguide loss. The waveguide losses can be estimated from the net modal gain spectra of Fig. 3. The modal gains converge to an almost constant value independent of the injection current density in the wavelength region greater than 1200 nm. In this region, the optical absorption due to the QDs when the TE and TM modes are propagating in the waveguide is negligible because the photon energy is lower than the ground-state energy of the QDs. Thereby, the constant gain value in the longer wavelength region corresponds to the waveguide loss. The estimated waveguide losses are approximately −14.6 and −19.3 cm^{-1} for the TE and TM components, respectively. As the polarization anisotropy of the confinement factor is too small to interpret the TE-polarized gain in Fig. 3, it is supposed to be dominantly caused by the anisotropic material gain and waveguide loss.

V. POLARIZATION CHARACTERISTICS OF 1000-μm CAVITY-LENGTH DEVICE

Next, we discuss the characteristics of the laser device with a cavity length of 1000 μm. Figures 4(a) and 4(b) show the Fabry–Pérot resonances of the TE and TM components, respectively, as a function of the injection current density. This device exhibits ground-state laser oscillation in both the TE and TM components. When the injection current density is 100 A/cm^2, the Fabry–Pérot resonances exhibit multiple

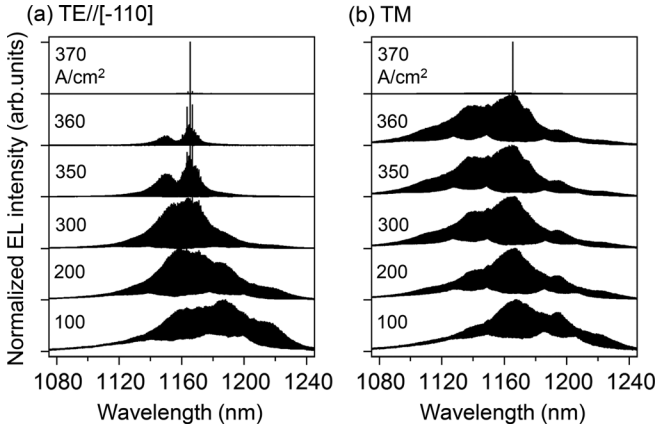

FIG. 4. Fabry–Pérot resonances of (a) the TE and (b) the TM polarization components obtained from the [−110] waveguide device with a 1000-μm cavity length, as functions of the injection current density.

peaks at around 1160, 1180, and 1220 nm for the TE component and at around 1140, 1160, and 1180 nm for the TM component. These multiple peaks arise from the constructive interference of the multi-mode optical propagation in the waveguide. All the peaks are due to emission from the inhomogeneously distributed ground states of the stacked QDs. In addition, bumps originating from the destructive interference of the multi-mode optical propagation, as mentioned in Sec. IV, appear on the bases of the resonance spectra. As the injection current density is increased, the peak at around 1160 nm become dominant in both the TE and TM spectra and the bumps gradually disappear, which indicates an enhancement of single-mode propagation. Then, the TE and TM spectra exhibit laser oscillation from the ground state of 1167 nm at 360 and 370 A/cm^2, respectively. Therefore, TM-laser oscillation can be achieved even from the ground state by adjusting the structural parameters such as device length, which leads to a threshold current density for laser oscillation lower than that for the 300-μm cavity-length device.

The polarization characteristics of the EL intensity and net modal gain also differ according to the cavity length. The polarization-angle dependence of the EL peak intensities represented by log-scale polar plots for various injection current densities is shown in Fig. 5. The polar plot shows an almost isotropic characteristic at 100 A/cm^2 because of the HH-LH mixing in the closely stacked QDs. As the injection

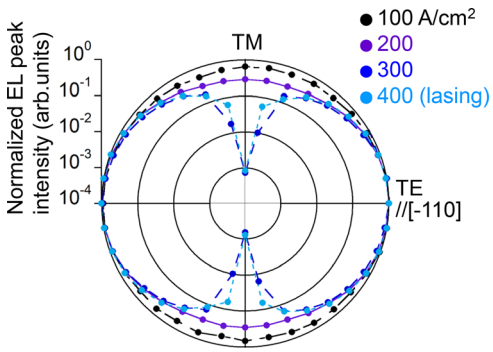

FIG. 5. Polarization-angle dependence of the EL peak intensities of the QD ground state for various injection current densities, which is represented as a log-scale polar plot.

current density is increased, the TE-emission intensity becomes dominant compared with the TM-emission intensity. This behavior is the same as that for the 300-μm cavity-length device, whereas the polarization anisotropy is significantly large at around the threshold current density for laser oscillation. As the inhomogeneous mode distribution of the TE spectrum becomes narrower for the 1000-μm cavity-length device exhibiting only ground-state emission, the concentration of the injected carriers on a certain mode of the TE component is enhanced. This results in a lower threshold current density for TE-laser oscillation than for TM-laser oscillation.

Figures 6(a) and 6(b) show the net modal gain spectra of the TE and TM components derived using the Hakki-Paoli method, respectively, as a function of the injection current density. The gain spectra have multiple peaks due to the multi-mode optical propagation. These peaks appear at the wavelength corresponding to the antinodes observed in the Fabry–Pérot resonance in Figs. 4(a) and 4(b). In the Hakki-Paoli method, the net modal gain is calculated by analyzing the Fabry–Pérot resonance obtained from a single-mode optical propagation, in which the base of the resonance is almost constant. In contrast, as the Fabry–Pérot resonance obtained from the multi-mode optical propagation has a bumpy base, the values of γ in Eq. (3) are underestimated at the dips of the resonance spectrum, which result in multiple peaks in the gain spectrum. The TE and TM modal gains at around 1160 nm gradually approach 0 cm^{-1} with increasing injection current density. When the modal gain becomes positive above 350 and 370 A/cm^2 for the TE and TM components, TE- and TM-laser oscillation occurs, respectively. Note that the TM modal gain spectrum exhibits a low signal-to-noise ratio at 370 A/cm^2 because very little Fabry–Pérot resonance is observed after laser oscillation. The threshold current densities for TE- and TM-laser oscillation are less than those of the 300-μm cavity-length device. As a longer cavity length results in a lower mirror loss per unit length represented in Eq. (4), the modal gain of the ground state becomes positive before ground-state filling, which leads to a lower threshold current density. The estimated waveguide losses are approximately -6.3 and $-9.6\,cm^{-1}$ for the TE and TM components, respectively, which are smaller than the waveguide losses of the 300-μm cavity-length device. Based on the comparison of the waveguide losses between the TE and TM components in the 300- and 1000-μm cavity-length devices, in order to achieve polarization-insensitivity at high net modal gain, we need to further improve the TM material gain by narrowing the inhomogeneous mode distribution due to the height fluctuation in the stacked QDs and compensate the waveguide loss for the TM component larger than that of the TE component.

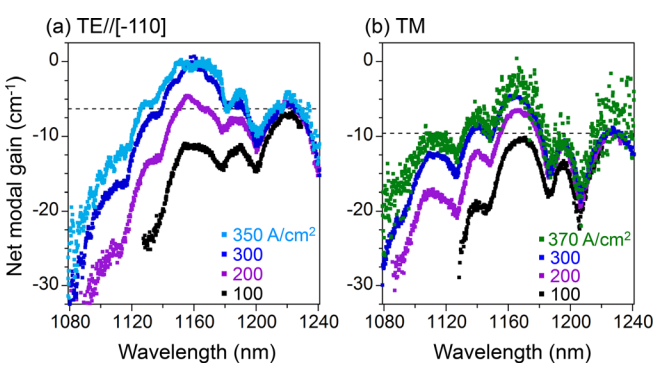

FIG. 6. Net modal gain spectra of (a) the TE and (b) the TM components derived from the Fabry–Pérot resonances in Figs. 4(a) and 4(b) by using the Hakki-Paoli method, respectively, as functions of the injection current density. The dashed lines represent the estimated mirror losses.

VI. SUMMARY

We studied the polarization anisotropy of the EL and net modal gain characteristics of laser device structures containing 40 stacked InAs/GaAs QD layers. As the HH-LH mixing caused by electronic coupling between the closely stacked QDs enhanced the TM polarization component, the [110] waveguide devices exhibited laser oscillation of not only the TE component but also the TM component. The wavelengths of laser oscillation differed according to the cavity length, i.e., laser oscillation at 1167 and 1137 nm from the ground state for the 1000-μm cavity-length device and the first excited state for the 300-μm cavity-length device, respectively. The polarized EL intensity exhibited an almost isotropic characteristic for a low injection current density, whereas it exhibited markedly TE-dominant anisotropy at around the threshold current density for laser oscillation. The net modal gain evaluated using the Hakki-Paoli method also exhibited a TE-enhanced characteristic with increasing injection current density. These anisotropic characteristics are caused by higher material gain due to the narrower inhomogeneous mode distribution and smaller waveguide loss in the TE component than in the TM component.

ACKNOWLEDGMENTS

We thank Dr. M. Ekawa of Fujitsu Laboratories, Ltd., for processing devices used in this work. This work was partially supported by a Grant-in-Aid for Scientific Research (No. 24360121) from the Ministry of Education, Culture, Sports, Science and Technology, Japan.

[1]D. Bimberg, M. Grundmann, and N. N. Ledentsov, *Quantum Dot Heterostructures* (Wiley, New York, 1998), Chap. 8.
[2]M. Sugawara, in *Semiconductors and Semimetals*, edited by M. Sugawara (Acamedic, San Diego, CA, 1999), Vol. 60, Chap. 6.
[3]M. Sugawara, N. Hatori, M. Ishida, H. Ebe, Y. Arakawa, T. Akiyama, K. Otsubo, T. Yamamoto, and Y. Nakata, J. Phys. D: Appl. Phys. **38**, 2126 (2005).
[4]M. Sugawara, H. Ebe, N. Hatori, M. Ishida, Y. Arakawa, T. Akiyama, K. Otsubo, and Y. Nakata, Phys. Rev. B **69**, 235332 (2004).
[5]E. W. Bogaart, R. Notze, Q. Gong, J. E. M. Haverkort, and J. H. Wolter, Appl. Phys. Lett. **86**, 173109 (2005).
[6]A. Marti, E. Antolin, C. R. Stanley, C. D. Farmer, N. Lopez, P. Diaz, E. Canovas, P. G. Linares, and A. Luque, Phys. Rev. Lett. **97**, 247701 (2006).
[7]A. H. Gnauck, G. Charlet, P. Tran, P. J. Winzer, C. R. Doerr, J. C. Centanni, E. C. Burrows, T. Kawanishi, T. Sakamoto, and K. Higuma, J. Lightwave Technol. **26**, 79 (2008).
[8]N. Yamamoto and H. Sotobayashi, "All-band photonic transport system and its device technologies," Proc. SPIE **7235**, 72350C (2009).
[9]N. Yamamoto, H. Sotobayashi, K. Akahane, M. Tsuchiya, K. Takashima, and H. Yokoyama, Opt. Express **16**, 19836 (2008).
[10]K. Kurokawa, K. Tsujikawa, K. Tajima, K. Nakajima, and I. Sankawa, "10 Gb/s WDM transmission at 1064 and 1550 nm over 24 km PCF with negative power penalties," in *Proceedings of the 12th Optoelectronics and Communications Conference, Yokohama, Japan* (2007), pp. 12C1–12C3.

[11]B. I. Miller, U. Koren, M. A. Newkirk, M. G. Young, R. M. Jopson, R. M. Derosier, and M. D. Chien, IEEE Photonics Technol. Lett. **5**, 520 (1993).
[12]P. Jayavel, H. Tanaka, T. Kita, O. Wada, H. Ebe, M. Sugawara, J. Tatebayashi, Y. Arakawa, Y. Nakata, and T. Akiyama, Appl. Phys. Lett. **84**, 1820 (2004).
[13]T. Kita, O. Wada, H. Ebe, Y. Nakata, and M. Sugawara, Jpn. J. Appl. Phys., Part 2 **41**, L1143 (2002).
[14]T. Kita, N. Tamura, O. Wada, M. Sugawara, Y. Nakata, H. Ebe, and Y. Arakawa, Appl. Phys. Lett. **88**, 211106 (2006).
[15]T. Saito, H. Ebe, Y. Arakawa, T. Kakitsuka, and M. Sugawara, Phys. Rev. B **77**, 195318 (2008).
[16]N. Yasuoka, K. Kawaguchi, H. Ebe, T. Akiyama, M. Ekawa, S. Tanaka, K. Morito, A. Uetake, M. Sugawara, and Y. Arakawa, Appl. Phys. Lett. **92**, 101108 (2008).
[17]K. Kawaguchi, N. Yasuoka, M. Ekawa, H. Ebe, T. Akiyama, M. Sugawara, and Y. Arakawa, Appl. Phys. Lett. **93**, 121908 (2008).
[18]P. Podemski, G. Sęk, K. Ryczko, J. Misiewicz, S. Hein, S. Höfling, A. Forchel, and G. Patriarche, Appl. Phys. Lett. **93**, 171910 (2008).
[19]T. Inoue, M. Asada, N. Yasuoka, O. Kojima, T. Kita, and O. Wada, Appl. Phys. Lett. **96**, 211906 (2010).
[20]Y. Ikeuchi, T. Inoue, M. Asada, Y. Harada, T. Kita, E. Taguchi, and H. Yasuda, Appl. Phys. Express **4**, 062001 (2011).
[21]M. Usman, T. Inoue, Y. Harada, G. Klimeck, and T. Kita, Phys. Rev. B **84**, 115321 (2011).
[22]A. Takahashi, T. Ueda, Y. Bessho, Y. Harada, T. Kita, E. Taguchi, and H. Yasuda, Phys. Rev. B **87**, 235323 (2013).
[23]T. Kita, M. Suwa, T. Kaizu, and Y. Harada, J. Appl. Phys. **115**, 233512 (2014).
[24]D. Hofstetter and R. L. Thornton, IEEE J. Quantum Electron. **34**, 1914 (1998).
[25]J. Kim and S. L. Chuang, IEEE J. Quantum Electron. **42**, 942 (2006).
[26]B. Hakki and T. L. Paoli, J. Appl. Phys **46**, 1299 (1975).
[27]E. V. Arzhanov, A. P. Bogatov, V. P. Konyaev, O. M. Nikitian, and V. I. Shveikin, Quantum Electron. **24**, 581 (1994).
[28]L. Harris, A. D. Ashmore, D. J. Mowbray, M. Hopkinson, G. Hill, and J. Clark, Appl. Phys. Lett. **75**, 3512 (1999).
[29]M. Sugawara, K. Mukai, Y. Nakata, H. Ishikawa, and A. Sakamoto, Phys. Rev. B **61**, 7595 (2000).
[30]D. Watanabe, N. Kasamatsu, Y. Harada, and T. Kita, Appl. Phys. Lett. **105**, 171904 (2014).
[31]V. G. Stolerua, D. Palb, and E. Towe, Physica E **15**, 131 (2002).
[32]S. Anantathanasarn, P. J. van Veldhoven, T. J. Eijkemans, T. de Vries, E. Smalbrugge, E. J. Geluk, E. A. J. M. Bente, Y. S. Oei, M. K. Smit, and R. Notzel, Appl. Phys. Lett. **92**, 123113 (2008).
[33]T. Kotani, S. Birner, P. Lugli, and C. Hamaghchi, J. Appl. Phys. **115**, 143501 (2014).
[34]T. Saito, T. Nakaoka, T. Kakitsuka, Y. Yoshikuni, and Y. Arakawa, Physica E **26**, 217 (2005).